We are IntechOpen,
the world's leading publisher of Open Access books
Built by scientists, for scientists

6,900
Open access books available

186,000
International authors and editors

200M
Downloads

154
Countries delivered to

Our authors are among the

TOP 1%
most cited scientists

12.2%
Contributors from top 500 universities

CLARIVATE ANALYTICS
BOOK CITATION INDEX
INDEXED

WEB OF SCIENCE™

Selection of our books indexed in the Book Citation Index
in Web of Science™ Core Collection (BKCI)

Interested in publishing with us?
Contact book.department@intechopen.com

Numbers displayed above are based on latest data collected.
For more information visit www.intechopen.com

Functional Tapered Fiber Devices Using Polymeric Coatings

Oscar González-Cortez, Rodolfo A. Carrillo-Betancourt,
Juan Hernández-Cordero and Amado M. Velázquez-Benítez

Abstract

A wide variety of fiber devices can be created by adding special coatings on tapered sections of optical fibers. In this work we present the fundamentals for the fabrication of tapered optical fibers coated with functional polymers. The required aspects of light propagation in tapered sections of optical fibers are introduced and the relevant parameters enabling light interaction with external media are discussed. A special case of interest is the addition of polymeric coatings with prescribed thicknesses in the tapered sections allowing for adjusting the light propagation features. We assess the use of liquid polymer coatings with varying thicknesses along the taper profile that can be tailored for tuning the transmission features of the devices. Hence, we introduce a methodology for obtaining coatings with predefined geometries whose optical properties will depend on the polymer functionality. As demonstrated with numerical simulations, the use of functional polymer coatings in tapered optical fibers allows for obtaining a wide variety of functionalities. Thus, controlled polymer coating deposition may provide a simple means to fabricate fiber devices with adjustable transmission characteristics.

Keywords: Tapered fibers, thin coatings, polymers, evanescent wave

1. Introduction

Optical fiber-based devices and sensors have been widely used in many fields of science and technology for different applications. In most applications, the transmission of light through in-line fiber devices is modified by an external perturbation and this can be quantified through variations in one or more characteristic features of the guided optical wave. Although extrinsic interaction of the light with the surrounding media is possible, the use of the evanescent portion of the guided wave offers some advantages. Exposure of the optical wave to the surrounding media in specific sections of the optical fibers is usually done by two alternatives [1–5]: removing the cladding material, or upon tapering a section of the optical fiber. The latter is the preferred approach to expose the evanescent wave since it involves a simple and reproducible process yielding low-loss devices. Although the description and basics of tapering optical fibers have been described since early 1990's by Birks *et al.* [1], new applications for these devices have been a subject of research due to their potential use in many fields of science and technology. Some of these applications include physical and biomedical sensing [6–10], interferometry [11],

excitation of surface plasmons [12, 13], atom detection [14, 15], and light coupling to micro-resonators [8, 16], just to name a few.

Tapering techniques and systems have evolved over the years resulting in optimized devices and standardized processes. As a result, tapering of optical fibers has been employed for modifying the light propagation conditions in fibers, and further allowing for the guided light to interact with other structures or materials. The latter capabilities allow for creating fiber-based devices incorporating coatings with controlled thicknesses and different optical properties. In this chapter we present the main aspects and basic guidelines for achieving a proper guidance of light through tapered devices providing also adequate interaction with the surrounding medium.

1.1 Basics of light propagation in optical fibers

Light propagation in optical fibers occurs within the fiber core (radius a) following the total internal reflection condition from Snell's law. Propagation conditions are defined by the physical characteristics of the core and cladding sections of the fiber: refractive indices and diameters. Due to the cylindrical geometry of the optical fibers and the small refractive index difference between the core and cladding materials, the propagating modes are obtained in a cylindrical coordinate system (r, φ, ϕ) and in terms of Bessel equations [17, 18]. Rigorous analysis and proper boundary conditions are used to obtain mathematical expressions describing the components of the electric and magnetic fields for the core ($r \leq a$) and the cladding ($r \geq a$) regions. The combination of these propagating fields allows for an alternative description in terms of linearly polarized modes, denoted as LP_{lm}, in which l and m are respectively the axial and radial indices. As an example, the electric field for the set of LP_{0m} modes can be shown to be given by:

$$
E_{LP_{0m}} = \begin{cases} E_0 J_0\left(\dfrac{u\,r}{a}\right), & r \leq a \\[4mm] E_0 \dfrac{J_0(u)}{K_0(w)} K_0\left(\dfrac{w\,r}{a}\right), & r > a \end{cases}, \tag{1}
$$

where E_0 is the field amplitude, J_0 is the zeroth-order Bessel function of the first kind, and K_0 is the zeroth-order modified Bessel function of the second kind. The parameters u and w are respectively the normalized propagation and attenuation constants, defined as:

$$
u = a\sqrt{k^2 n_{core}^2 - \beta^2}, \quad w = a\sqrt{\beta^2 - k^2 n_{cladd}^2}, \tag{2}
$$

involving the propagation constant of the guided wave (β), the wave number (k) and the refractive indices of the core (n_{core}) and the cladding (n_{cladd}). The description in terms of the LP_{lm} modes is very useful as these can be experimentally observed as intensity patterns (I_{lm}) whose mathematical representations are [17]:

$$
I_{lm} = \begin{cases} I_0 J_l^2\left(\dfrac{u\,r}{a}\right) \sin^2(l\phi), & r \leq a \\[4mm] I_0 \left(\dfrac{J_l(u)}{K_l(w)}\right)^2 K_l^2\left(\dfrac{w\,r}{a}\right) \sin^2(l\phi), & r > a \end{cases}. \tag{3}
$$

Another important parameter to assess the modal features of an optical fiber is the normalized frequency or V number, defined as:

$$V = \sqrt{u^2 - w^2} = \frac{2\pi a \sqrt{n_{core}^2 - n_{cladd}^2}}{\lambda}. \tag{4}$$

The normalized frequency is typically used as an indicator of how many modes are supported by the fiber. It can be shown that standard single mode fibers (SMFs) supporting only the fundamental (LP_{01}) mode have a $V < 2.405$. Hence, this condition is typically used as an indicator of single-mode propagation in an optical fiber.

1.2 Light propagation in tapered optical fibers

Tapered optical fibers are fabricated such that the physical dimensions of the core and cladding are reduced, thereby modifying the light propagation conditions [8, 19, 20]. The implication of this reduction in the physical dimensions of the fiber is a decrease in the effective refractive index of the core and thus a change in the light confinement. An effect caused by the core reduction is the compression of the light inside the core, although the evanescent wave increases in magnitude. However, there is a physical limit for the core reduction since the light cannot be effectively guided inside this region under certain conditions. After reaching this "guiding threshold" in the dimensions of the core, light escapes to the cladding material, which acts as the new core of the optical fiber while the surrounding media becomes the new cladding. As a consequence, the evanescent wave is effectively exposed to the external medium, granting the possibility of light interaction with different materials or structures.

Typically, tapered optical fibers are segmented in three sections for their analysis [1]: *the non-tapered segment of the optical fiber*, the *transition* and the *waist sections*, as depicted in **Figure 1a**. The waist section of the fiber is where the fiber is tapered down to its final diameter after which it remains constant across all its length. Usually, the interaction or coupling to other structures or materials takes place at this section. The transition sections of the fiber are those at which the diameter goes from the original diameter to the tapered section, and vice versa. Although the transition regions are commonly not used for sensing or coupling, they are significantly important as disturbances or non-desired alterations to light can occur in these sections. Such effects appear when the transition between diameters is not smooth or non-adiabatic.

Adiabaticity criteria comes from the tapering angle, which must be small enough for the fundamental mode to smoothly propagate across all the sections with minimal power loss [19]. Any sudden change in the dimensions or geometry of the fiber will provoke imminent light leaking from the core. This is avoided by performing the tapering process at a very slow rate. Considering the case of tapering a SMF, an adequate transition should maintain the fundamental mode through all the sections of the tapered fiber with negligible losses. Conversely, a non-adiabatic tapering
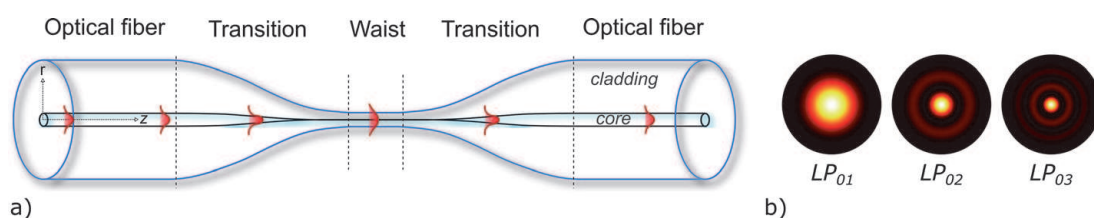

Figure 1.
(a) Tapered optical fiber profile indicating the three zones: non-tapered, transition and waist. (b) Intensity distributions of the LP_{om} *modes excited in the transition section and propagating in the waist of the taper.*

process will produce a "leakage" of light into the cladding exciting higher order modes.

The parameter used to define the adiabaticity of the tapered fiber is the *local length-scale* of the taper (z_t), resulting from the ratio of the core radius (r) over the tapering angle (Ω), expressed as $z_t = \frac{r}{\Omega}$. Notice that both variables (r and Ω) vary with length, i.e., $r = r(z)$ and $\Omega = \Omega(z)$ [19]. To achieve adiabaticity, the length of the taper must be larger than the length required to couple the fundamental mode to the predominant cladding mode. This coupling length is given by the beat length (z_b), which in turn depends on the propagation constant, $\beta = k n_{eff}$, with $k = \frac{2\pi}{\lambda}$. Thus, this variable is given by the expression [19]:

$$z_b = \frac{2\pi}{\beta_1 - \beta_{CM}},$$

(5)

where β_1 is the propagation constant of the fundamental LP_{01} mode, and β_{CM} corresponds to the propagation constant of the excited cladding mode. In an axially symmetric tapered fiber, the fundamental mode will only couple to azimuthally symmetric higher order modes (i.e., the LP_{0m} modes) supported by the cladding structure (see **Figure 1b**).

To illustrate the phenomena related to tapering optical fibers, we will use as an example a step-index standard single-mode silica fiber with core radius of 4.1 μm, cladding radius of 62.5 μm and refractive index difference $\Delta n = 0.061$. These are typical dimensions for the standard telecommunication fibers that are commonly used for the fabrication of tapered fibers for evanescent coupling of light to other photonic devices. Upon considering an adiabatic tapering process, firstly can be noticed that by reducing the core radius the V number is also modified. This implies that the effective refractive index (n_{eff}) of the waveguide will be modified as well and thus the propagation constant. The solutions in terms of the Bessel approximations yield the values of the propagation constants (β) resulting from these changes in geometry [17, 18]. **Figure 2** shows results from numerical calculations illustrating that a reduction in the propagation constant is obtained as the core radius decreases. Notice also that for $V < 1$, a sudden decrease in β occurs indicating that light cannot be longer confined in the core and hence it couples to the cladding material. Such
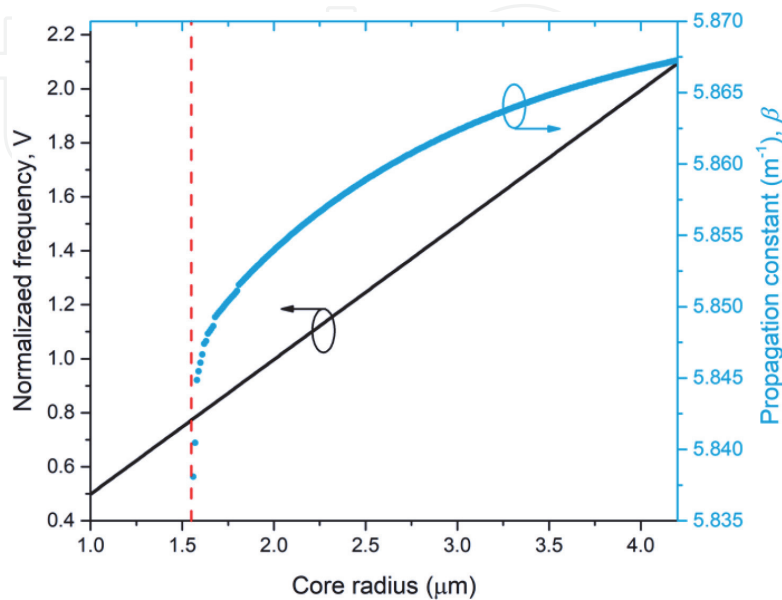

Figure 2.
Variation of the normalized frequency (V) and propagation constant (β) for different core radii corresponding to different tapering ratios. The dashed line shows the "guiding threshold" of the fiber core.

phenomenon implies that the whole material of the optical fiber, core and cladding, acts together as the new core of the waveguide, while the surrounding medium serves as the new cladding. The first reports on this phenomenon mention values for this guiding threshold V_{TH} near 0.8 [8, 19] to achieve this condition. Our numerical results indicate that light confinement in the fiber core is sustained until $V_{TH} \approx 0.77$, which corresponds to an approximate core radius of 1.55 μm, as illustrated in **Figure 2**.

The intensity distribution of the fundamental mode is modified as the fiber is tapered. For core diameters above the guiding threshold, a tighter confinement of light within the core is achieved. However, the amount of light in the evanescent portion of the wave increases and so its extension inside the cladding. Once the guiding threshold is surpassed, light confinement shifts from the core to the cladding, distributing across the entire waist material. This effect is illustrated in **Figure 3**, showing light confinement at different tapering ratios. Instantly, as the guided light is exposed to the external media, light confinement and propagation are determined by the surrounding materials. At this stage, interaction with the surrounding media occurs via the evanescent wave. Nonetheless, the amount of light exposed to the external media can be tailored by defining the final waist diameter. For a fiber surrounded by air, due to the large refractive index difference with respect to the silica, the *V* number substantially increases allowing to reduce the fiber core down to very small diameters. Subwavelength waist diameters have been reported for tapered fiber devices in sensing and other applications [8, 15, 21].

The wavelength of light is also relevant in this phenomenon as in every waveguiding structure. Light confinement in the fundamental mode will change depending on the wavelength, showing a larger amount of evanescent wave for
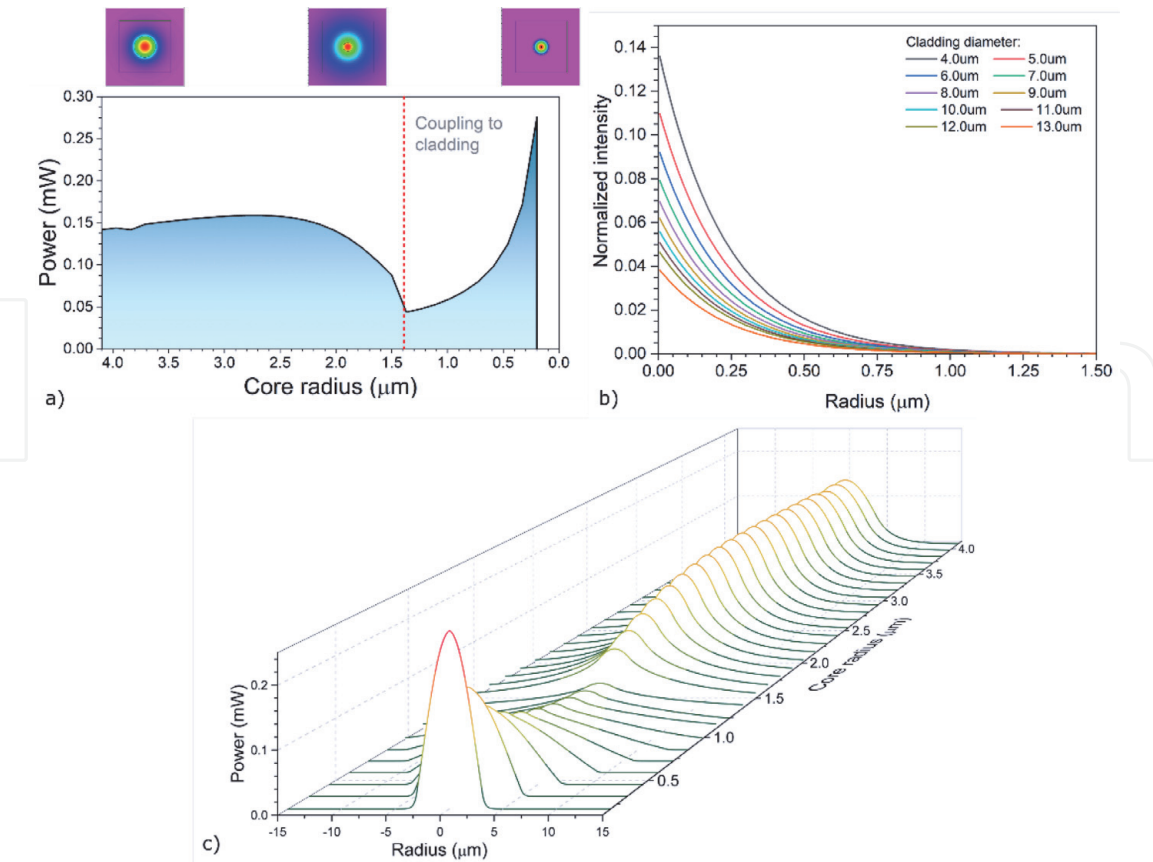

Figure 3.
Light confinement in tapered optical fibers. Fundamental mode power evolution at different core radii corresponding to different tapering ratios: (a) peak power and (b) power distribution. (c) Evanescent wave extension for different tapering ratios.
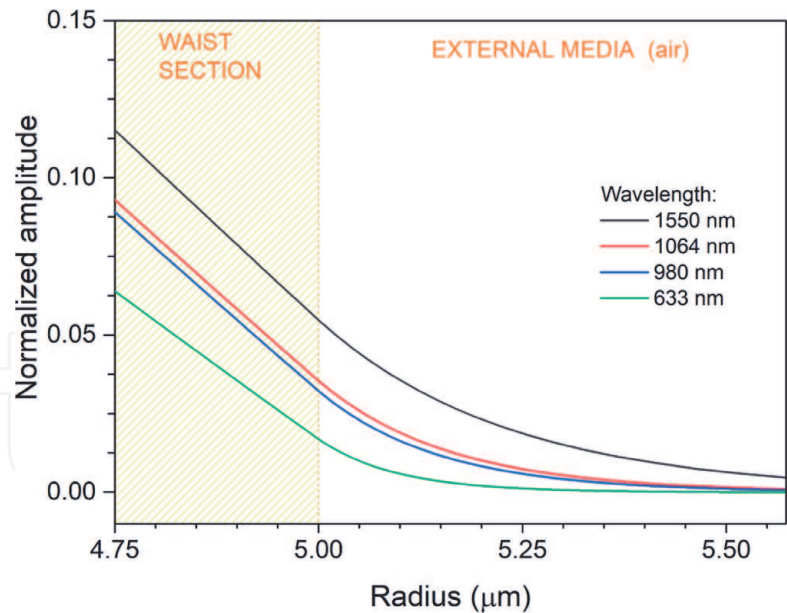
Figure 4.
Wavelength dependence of the penetration of the evanescent wave of the fundamental mode to external media at the waist of a tapered optical fiber.

longer wavelengths. Assuming an adiabatically tapered SMF with a 5 μm waist radius with air as the surrounding medium, the extension of the evanescent wave will present a significant increase as illustrated in **Figure 4**. Hence, for a given tapered device with specific dimensions, wavelength selection is essential as this will change the exposure and hence the interaction of the evanescent wave with the external medium.

Light exposure through evanescent wave is useful for the creation of functional devices by means of adding different materials as coatings. The amount of evanescent wave exposed to the surrounding media determines the range of coating thicknesses that can be effectively used for efficient interaction depending on the materials as well. The fundamentals of fiber coating and main aspects to consider for the creation of devices using diverse materials as coatings are discussed in the following sections.

2. Fiber coating

There are multiple reports using diverse techniques for coating optical fibers with tapered sections. We will focus on a method based on the deposition of liquid materials over specific sections of optical fibers since these are convenient for post-processing fibers. We consider in particular the use of liquid polymers as coating materials, since they offer a wide variety of functionalities. Polymers have been used for recoating fiber devices such as Bragg gratings, amplifiers or splices, just to mention the most important. Various works have demonstrated the effectiveness of using this technique for diverse purposes [22–25], and recoating systems to perform such task have been readily reported [26].

The process for deposition of controlled layer coatings on optical fibers using liquid materials, such as polymers, are suitably described by the wire coating technique [27–29]. This involves the immersion of the fiber into the liquid and retrieve it at a prescribed speed to obtain a desired thickness, as illustrated in **Figure 5**. The main factors involved in this process include the characteristics of the liquid such as viscosity (η) and surface tension (γ), and the velocity (v) at which the process takes
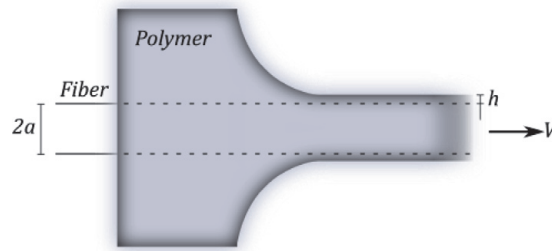
Figure 5.
Wire coating technique scheme. A layer of coating material (thickness h) is left on the surface of the wire (radius a) by pulling the coating material at a constant velocity (v) through a liquid container.

place. The ratio of the viscosity to the surface tension, multiplied by the velocity of the coating process, is defined as the capillary number, which allows to compare the behavior of different liquids. This ratio is a dimensionless number defined explicitly as $Ca = \eta v/\gamma$. For liquids with $Ca << 1$, the resulting coating thickness (h) deposited on a fiber of radius (a) can be obtained as [29]:

$$h = 1.34 a Ca^{2/3}. \tag{6}$$

This expression holds only for $Ca < 1$ since the fluid dynamics are different for larger values of the capillary number. Nonetheless, proper adjustments to this theory can be made yielding a correction factor for the thickness [30]. This wire coating theory has been largely investigated and described in the field of fluidics describing in detail multiple scenarios and materials.

Given the nature of the liquids, an additional factor to consider for their use as fiber coatings is the Rayleigh-Plateau instability [31]. This effect leads to the breakdown of the uniform layer into a periodic array of droplets. Such behavior will always occur at characteristic time (t_0) given by:

$$t_0 = 12 \frac{\eta(r+a)^4}{\gamma h^3}. \tag{7}$$

This is an important effect that must be considered when applying liquid coatings because it indicates the maximum time in which the liquid layer will remain with a uniform thickness. Therefore, the coating must be solidified before this characteristic time in order to preserve its shape. Hence, different polymeric materials cured by means of chemical, thermal or photo-active processes must account for this breakdown time.

3. Coatings on tapered optical fibers

In most cases, the coatings on the tapered sections of the fiber are sought to be with uniform thickness in order to obtain interaction with the evanescent wave. Ideally, only the waist section of the taper should be coated, as indicated in the green region in **Figure 6a**. However, there are two aspects that must be also considered when designing the coating: the actual exposition of the evanescent wave and the coating process itself. In practice, coating only the waist section of the tapered fiber might represent a challenging task since the liquid to be deposited is usually contained within a reservoir with prescribed dimensions that do not match the length of the waist. Extraction of the fiber from the reservoir can also be a potential factor to
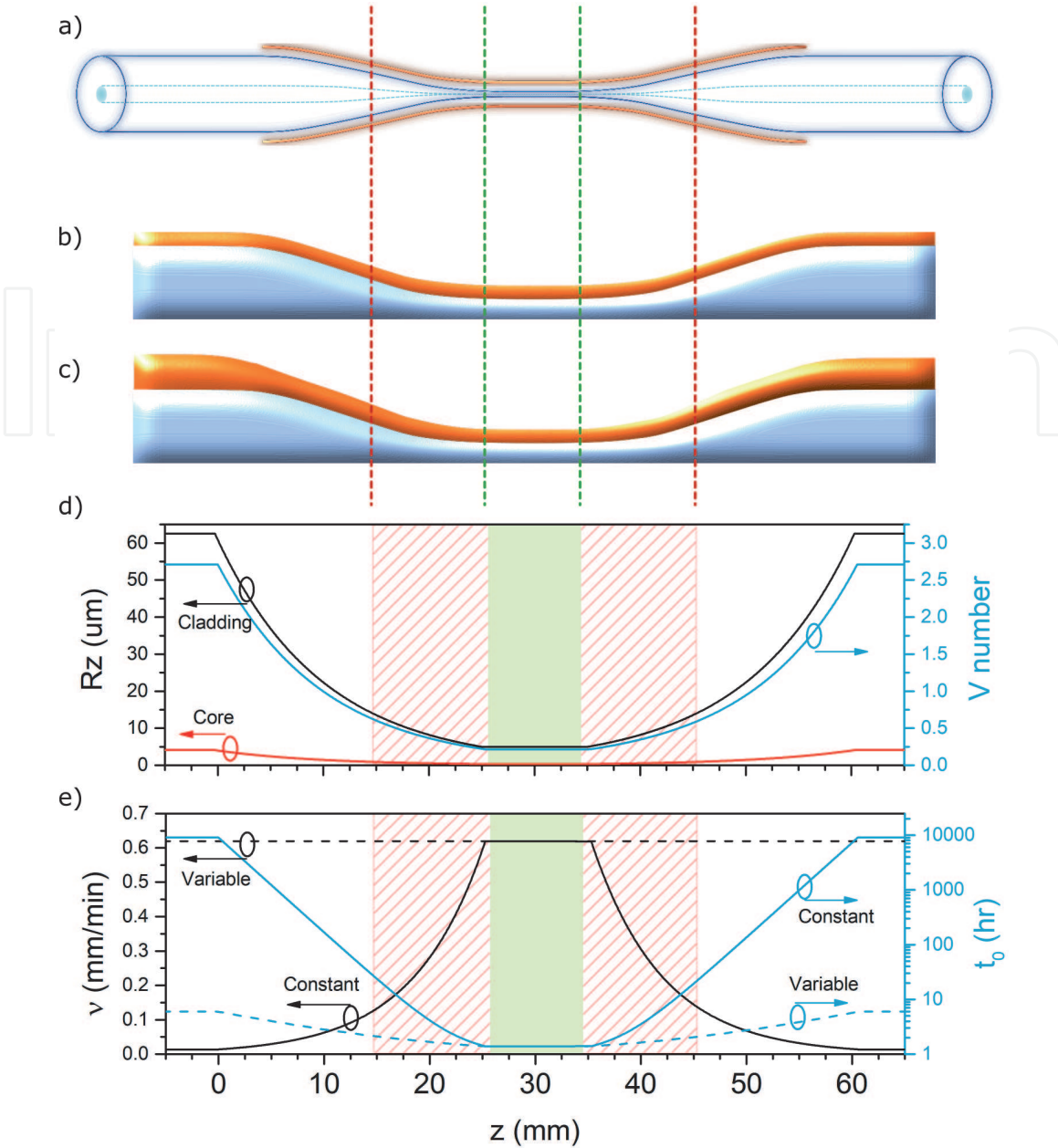
Figure 6.
Coatings on optical fibers. (a) Schematic of a coated tapered optical fiber in different regions showing the regions where coupling from the core to the cladding occurs and the modal distribution in the waist section. (b) Constant and (c) variable thickness coatings along the tapered fiber. (d) Variation of the normalized frequency (V number) of the fiber core along the taper; the red regions indicate the core-cladding coupling zones and light interacts with coating; the green zone indicates the uniform waist section. (e) Coating speeds (v) required to obtain constant and variable coating thicknesses along the taper; the plot includes the corresponding characteristic time (t_o) for the instabilities.

generate a non-uniform coating; this task is usually performed upon pulling the fiber from the non-tapered section and hence liquid is also deposited in other regions of the tapered fiber. The transition zones of the tapered fiber are therefore coated as well, and this minimizes any perturbations generated by the reservoir.

Non-uniformities in the coating thickness are a potential source of perturbation that may result in light leaking in the optical fiber. Given the variable radius profile of the tapered fiber and the radius dependency for the resultant thickness given by (6), the profile of the coating can be modified depending on the velocity of the process. Then, two scenarios can result from the coating process: a uniform coating along the entire fiber obtained upon adjusting the speed (**Figure 6b**), or a variable coating layer using a constant speed during the process (**Figure 6c**). In all cases, it is also important to consider the cross-linking mechanism of the coating polymer.

Once the coating is deposited, it might require a longer period of time for achieving solidification.

To exemplify these possibilities, we consider a tapered optical fiber coated with polydimethylsiloxane elastomer (PDMS, Sylgard 184 from Dow), which has a $\eta = 3.5[Pa \bullet s]$ and $\gamma = 0.0198[N \bullet m^{-1}]$ [26, 32]. For the SMF tapered down to a waist radius of 5 μm, the lengths of the waist and transitions are 10 and 25 mm, respectively; the transitions are assumed to have an exponential profile as described in [1]. For this specific fiber light couples into the cladding, and thus evanescent wave exposition into the surrounding media occurs along the transition section (red region in **Figure 6**). The radii of the fiber core and the cladding are compared with the modification of the normalized frequency in **Figure 6d**. The nature of the curing or solidifying process of the polymer is crucial and should be considered due to the possible appearance of instabilities. To avoid this, both the coating and curing processes needs to be shorter than the characteristic time (t_0) in the waist section.

PDMS is a polymer cured by heating, requiring from several minutes to hours for complete solidification, depending on the temperature of the curing process. For achieving a 200 nm thick uniform PDMS coating at the waist section, a speed coating process of around $\nu = 0.62[mm \bullet min^{-1}]$ is required, and the critical time is $t_0 = 1.4[hr]$. The conditions required for generating a coating with constant or variable thickness layers are analyzed in **Figure 6e**. For obtaining a coating with constant thickness (solid line), the required coating speed increases inversely with the fiber diameter. Although the instabilities mostly appear at larger times along the tapered fiber, the total duration of the process will be in general longer. In contrast, the variable coating (dashed line) implicates overall shorter times for instabilities to appear, and the process must be performed much faster.

Depending on the application, fiber coatings can be designed to optimize the interaction of the evanescent wave with the surrounding media. This means that the thickness of the coating can be extended to completely enclose the evanescent wave, or simply to favor some interaction and leave a remaining portion of light still interacting with the external media. Having this in mind, one must also consider the refractive index of the material: while low refractive index materials will require thinner coatings to completely isolate the evanescent wave, high refractive index
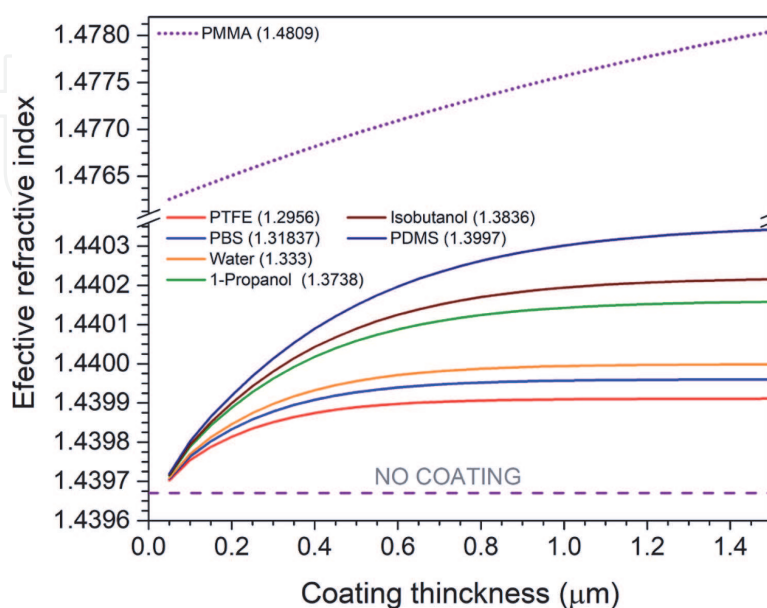

Figure 7.
Effective refractive index at the waist section of the fiber as a function of the coating thickness for materials commonly used for taper coating and for sensing applications: PTFE [33], PBS [34], water [34], 1-propanol [35], isobutanol [35] and PDMS [26, 32].
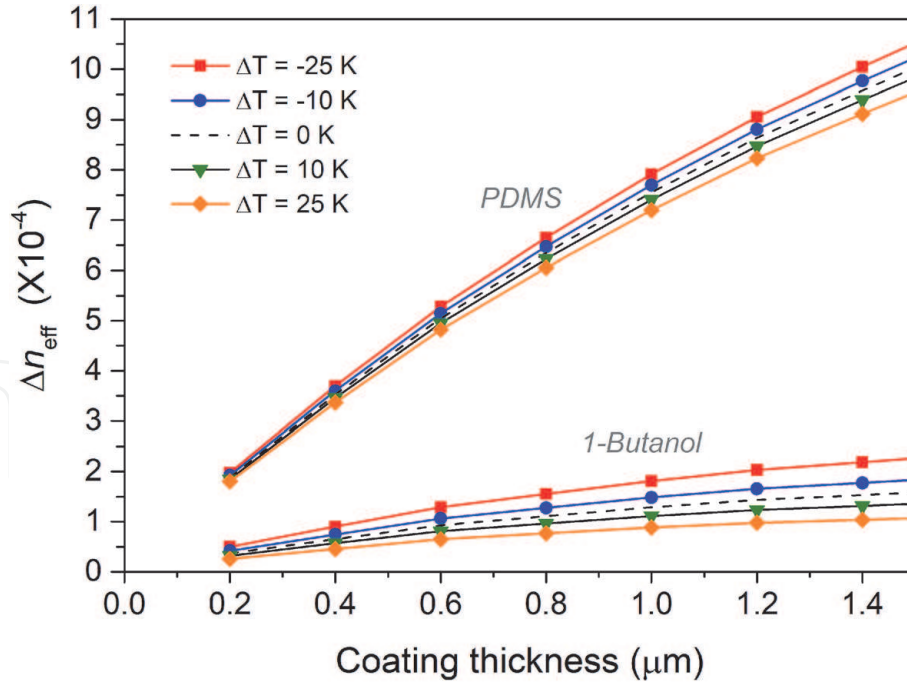
Figure 8.
Temperature dependence of the LP_{o1} mode effective refractive index (n_{eff}) for different thicknesses of PDMS coatings.

materials will allow to use thicker coatings before isolating the evanescent wave, as illustrated in **Figure 7**. Of course, to have efficient and low loss light propagation in the tapered fiber, the refractive index of the coating material must be lower than the refractive index of the optical fiber. Otherwise, this will induce losses since the light propagated in the cladding will never been coupled again the core.

4. Applications of coatings for devices

Different effects can be generated in the guided wave depending on the optical properties of the coating material. For instance, the sensitivity of the tapered device to physical parameters can be tailored up to some extent. Using again as an example PDMS coatings, the effective refractive index of the fundamental mode can be adjusted with the coating thickness. It is well known that PDMS experiences changes with temperature due to its thermal expansion coefficient and to its thermo-optic coefficient ($\Delta n/\Delta T \left[K^{-1} \right] = -1.8 \times 10^{-4}$) [32]. As the thickness of the PDMS coating is increased, the effective refractive index will increase its variation with temperature, as shown in **Figure 8**. Evidently, this "tunability" in sensitivity is limited, and it further depends on the thermo-optical properties of the polymer. To illustrate this, we have also included in **Figure 8** an example using 1-Butanol as the coating material [35]. Notice that in this case, lower effective indices are obtained and their variations with coating thickness are not as pronounced as obtained for PDMS. However, the sensitivity of the effective index to temperature changes for this coating is larger than that of PDMS.

5. Conclusions

We have introduced guidelines for coating tapered sections of optical fibers with liquid materials. Specifically, we undertake the subject of polymeric thin layers

deposited by the wire coating technique and the interaction of the coating with the evanescent wave. Firstly, the propagation considerations to achieve light interaction with the surrounding media via evanescent wave were described. This aspect depends on the physical dimensions, refractive indices of the materials and propagating wavelength. As shown upon analyzing the wire coating technique, it is possible to define parameter for the coating process that will allow for controlling the coating thickness and avoid coating instabilities. Essentially, once the properties of the liquid polymer and the dimensions of the taper are known, the coating velocity may be calculated in order to obtain a prescribed coating thickness. Finally, light propagation for different coating thickness with different materials was discussed in terms of the influence on the effective refractive index in the waist section of the fiber. These aspects should be of interest for obtaining photonic devices with functional polymers coatings that may be useful for sensing applications.

Acknowledgements

Conflict of interest

The authors declare no conflict of interest.

Author details

Oscar González-Cortez[1], Rodolfo A. Carrillo-Betancourt[1,2],
Juan Hernández-Cordero[2] and Amado M. Velázquez-Benítez[1*]

1 Instituto de Ciencias Aplicadas y Tecnología, Universidad Nacional Autónoma de México, Mexico City, Mexico

2 Instituto de Investigaciones en Materiales, Universidad Nacional Autónoma de México, Mexico City, Mexico

*Address all correspondence to: amado.velazquez@icat.unam.mx

IntechOpen

References

[1] Birks TA, Li YW. The shape of fiber tapers. Journal of Lightwave Technology. 1992 Apr;10(4):432-438. DOI: 10.1109/50.134196

[2] Baker, Chams, and Martin Rochette. "A generalized heat-brush approach for precise control of the waist profile in fiber tapers." Optical Materials Express 1.6 (2011): 1065-1076. DOI: 10.1364/OME.1.001065

[3] Haddock HS, Shankar PM, Mutharasan R. Fabrication of biconical tapered optical fibers using hydrofluoric acid. Materials Science and engineering: B. 2003 Jan 15;97(1):87-93. https://doi.org/10.1016/S0921-5107(02)00434-8

[4] Ko S, Lee J, Koo J, Joo BS, Gu M, Lee JH. Chemical wet etching of an optical fiber using a hydrogen fluoride-free solution for a saturable absorber based on the evanescent field interaction. Journal of Lightwave Technology. 2016 Aug 15;34(16): 3776-3784. DOI: 10.1109/JLT.2016.2583061

[5] Nikbakht, Hamed, Hamid Latifi, Mohammadreza Oraie, and Tahere Amini. "Fabrication of tapered tip fibers with a controllable cone angle using dynamical etching." Journal of Lightwave Technology 33, no. 23 (2015): 4707-4711. DOI: 10.1109/JLT.2015.2453365

[6] Villatoro, Joel, David Monzón-Hernández, and Efrain Mejía. "Fabrication and modeling of uniform-waist single-mode tapered optical fiber sensors." Applied optics 42, no. 13 (2003): 2278-2283. DOI: 10.1364/AO.42.002278

[7] Yang, Rui, Yong-Sen Yu, Cong-Cong Zhu, Yang Xue, Chao Chen, Xuan-Yu Zhang, Bao-Lin Zhang, and Hong-Bo Sun. "PDMS-coated S-tapered fiber for highly sensitive measurements of transverse load and temperature." IEEE Sensors Journal 15, no. 6 (2015): 3429-3435. DOI: 10.1109/JSEN.2015.2388490

[8] Brambilla G, Xu F, Horak P, Jung Y, Koizumi F, Sessions NP, Koukharenko E, Feng X, Murugan GS, Wilkinson JS, Richardson DJ. Optical fiber nanowires and microwires: fabrication and applications. Advances in Optics and Photonics. 2009 Jan 30;1 (1):107-161. https://doi.org/10.1364/AOP.1.000107

[9] Leung, Angela, P. Mohana Shankar, and Raj Mutharasan. "A review of fiber-optic biosensors." Sensors and Actuators B: Chemical 125, no. 2 (2007): 688-703. DOI: 10.1016/j.snb.2007.03.010

[10] Tian, Ye, Wenhui Wang, Nan Wu, Xiaotian Zou, and Xingwei Wang. "Tapered optical fiber sensor for label-free detection of biomolecules." Sensors 11, no. 4 (2011): 3780-3790. DOI: 10.3390/s110403780

[11] Yadav, T. K., R. Narayanaswamy, MH Abu Bakar, Y. Mustapha Kamil, and M. A. Mahdi. "Single mode tapered fiber-optic interferometer based refractive index sensor and its application to protein sensing." Optics Express 22, no. 19 (2014): 22802-22807. DOI: 10.1364/OE.22.022802

[12] Verma, Rajneesh K., Anuj K. Sharma, and B. D. Gupta. "Surface plasmon resonance based tapered fiber optic sensor with different taper profiles." Optics Communications 281, no. 6 (2008): 1486-1491. DOI: 10.1016/j.optcom.2007.11.007

[13] Monzón-Hernández, David, Joel Villatoro, Dimas Talavera, and Donato Luna-Moreno. "Optical-fiber surface-plasmon resonance sensor with multiple resonance peaks." Applied optics 43, no. 6 (2004): 1216-1220. DOI: 10.1364/AO.43.001216

[14] O'Shea, Danny, Christian Junge, Jürgen Volz, and Arno Rauschenbeutel. "Fiber-optical switch controlled by a single atom." Physical review letters 111, no. 19 (2013): 193601. DOI: 10.1103/ PhysRevLett.111.193601

[15] Wu X, Tong L. Optical microfibers and nanofibers. Nanophotonics. 2013 Dec 16;2(5–6):407-428. https://doi.org/ 10.1515/nanoph-2013-0033

[16] Monifi, Faraz, Sahin Kaya Özdemir, Jacob Friedlein, and Lan Yang. "Encapsulation of a fiber taper coupled microtoroid resonator in a polymer matrix." IEEE Photonics Technology Letters 25, no. 15 (2013): 1458-1461. DOI: 10.1109/LPT.2013.2266573

[17] Buck JA. Fundamentals of optical fibers. John Wiley & Sons; 2004 Apr 27.

[18] Okamoto K. Fundamentals of optical waveguides. Academic press; 2006.

[19] Love JD, Henry WM, Stewart WJ, Black RJ, Lacroix S, Gonthier F. Tapered single-mode fibres and devices. Part 1: Adiabaticity criteria. IEE Proceedings J (Optoelectronics). 1991 Oct 1;138(5): 343-354. DOI: 10.1049/ip-j.1991.0060

[20] Black, R. J., S. Lacroix, F. Gonthier, and J. D. Love. "Tapered single-mode fibres and devices. II. Experimental and theoretical quantification." IEE Proceedings J-Optoelectronics 138, no. 5 (1991): 355-364. DOI: 10.1049/ip-j.1991.0061

[21] Sumetsky, M. "Nanophotonics of optical fibers." Nanophotonics 2, no. 5-6 (2013): 393-406. DOI: 10.1515/nanoph-2013-0041

[22] Kakarantzas, George, Sergio G. Leon-Saval, T. A. Birks, and P. St J. Russell. "Low-loss deposition of solgel-derived silica films on tapered fibers." Optics letters 29, no. 7 (2004): 694-696. DOI: 10.1364/OL.29.000694

[23] Li, Bao-li, Jin-hui Chen, Fei Xu, and Yan-qing Lu. "Periodic micro-structures in optical microfibers induced by Plateau-Rayleigh instability and its applications." Optics express 25, no. 4 (2017): 4326-4334. DOI: 10.1364/ OE.25.004326

[24] Vélez-Cordero, J. Rodrigo, A. M. Velázquez-Benítez, and J. Hernández-Cordero. "Thermocapillary flow in glass tubes coated with photoresponsive layers." Langmuir 30, no. 18 (2014): 5326-5336. DOI: 10.1021/la404221p

[25] Xu, Z. Y., Y. H. Li, and L. J. Wang. "Versatile technique to functionalize optical microfibers via a modified sol-gel dip-coating method." Optics letters 39, no. 1 (2014): 34-36. DOI: 10.1364/ OL.39.000034

[26] Velázquez-Benítez, Amado M., Moisés Reyes-Medrano, J. Rodrigo Vélez-Cordero, and Juan Hernández-Cordero. "Controlled deposition of polymer coatings on cylindrical photonic devices." Journal of Lightwave Technology 33, no. 1 (2014): 176-182. DOI: 10.1109/JLT.2014.2377173

[27] Landau, Levich, and B. Levich. "Dragging of a liquid by a moving plate." In Dynamics of curved fronts, pp. 141-153. Academic Press, 1988. DOI: 10.1016/B978-0-08-092523-3.50016-2

[28] De Ryck, Alain, and David Quéré. "Inertial coating of a fibre." Journal of Fluid Mechanics 311 (1996): 219-237. DOI: 10.1017/S0022112096002571

[29] Quéré, David. "Fluid coating on a fiber." Annual Review of Fluid Mechanics 31, no. 1 (1999): 347-384. DOI: 10.1146/annurev.fluid.31.1.347

[30] White, David A., and John A. Tallmadge. "A theory of withdrawal of cylinders from liquid baths." AIChE Journal 12, no. 2 (1966): 333-339. DOI: 10.1002/aic.690120223

[31] Rayleigh, Lord. "On the instability of jets." Proceedings of the London mathematical society 1, no. 1 (1878): 4-13. DOI: 10.1112/plms/s1-10.1.4

[32] Li, Bei-Bei, Qing-Yan Wang, Yun-Feng Xiao, Xue-Feng Jiang, Yan Li, Lixin Xiao, and Qihuang Gong. "On chip, high-sensitivity thermal sensor based on high-Q polydimethylsiloxane-coated microresonator." Applied Physics Letters 96, no. 25 (2010): 251109. DOI: 10.1063/1.3457444

[33] Yang, Min K., Roger H. French, and Edward W. Tokarsky. "Optical properties of Teflon® AF amorphous fluoropolymers." Journal of Micro/ Nanolithography, MEMS, and MOEMS 7, no. 3 (2008): 033010. DOI: 10.1117/ 1.2965541

[34] Hoang, Van Thuy, Grzegorz Stępniewski, Karolina H. Czarnecka, Rafał Kasztelanic, Van Cao Long, Khoa Dinh Xuan, Liyang Shao, Mateusz Śmietana, and Ryszard Buczyński. "Optical properties of buffers and cell culture media for optofluidic and sensing applications." Applied Sciences 9, no. 6 (2019): 1145. DOI: 10.3390/app9061145

[35] Moutzouris, Konstantinos, Myrtia Papamichael, Sokratis C. Betsis, Ilias Stavrakas, George Hloupis, and Dimos Triantis. "Refractive, dispersive and thermo-optic properties of twelve organic solvents in the visible and near-infrared." Applied Physics B 116, no. 3 (2014): 617-622. DOI: 10.1007/ s00340-013-5744-3